Energy Conversion and Management 55 (2012) 49–59

Contents lists available at SciVerse ScienceDirect

Energy Conversion and Management

journal homepage: www.elsevier.com/locate/enconman

Dust deposition in ventilation and air-conditioning duct bend flows

Ran Gao, Angui Li *

School of Environmental and Municipal Engineering, Xi'an University of Architecture and Technology, Xi'an, Shaanxi 710055, PR China

ARTICLE INFO

Article history:
Received 4 December 2009
Received in revised form 22 October 2011
Accepted 22 October 2011
Available online 24 November 2011

Keywords:
Particles
Ventilation duct bends
Computational fluid dynamics
Lagrangian eddy lifetime model
Dimensionless deposition velocities of particles
Dimensionless relaxing time

ABSTRACT

Particles carried by airflows in ventilation and air-conditioning systems have adverse effects on the quality of air in buildings and hence the health of building occupants. Gaining insight on particle deposition onto ventilation and air-conditioning duct bends is important for controlling pollutant dispersion. Based on the Reynolds stress transport model (RSM), this paper has taken into account the effects of drag, lift force, gravity, inertia force, turbulent diffusions, particle size and air velocity on the dimensionless deposition velocity of particles in smooth duct bends using fully developed velocity profiles. At two different air velocities of 3.0 m/s and 7.0 m/s, the aforementioned effects were predicted by Reynolds-averaged Navier–Stokes (RANS)-Lagrangian simulation on square shaped duct bends with different ways of placement.

Preliminary results suggest that gravity and inertia force enhance the dimensionless deposition as dimensionless relaxation time rises. Change tendency of the dimensionless particle deposition velocity on different surfaces of bend duct agrees well with previous studies. As air velocity and particle diameter increase, a significant increase of particle deposition coefficient in the duct bends is observed. Particle deposition to intrados can be intensified by the combined action of gravity and inertia force in different direction.

1. Introduction

A number of problems associated with human health are caused by the particle deposition on ventilation and air-conditioning duct bend. Particles can deposit in and re-suspend from the duct surfaces. Re-suspension of particles may expose building occupants to high levels of particle concentration [1]. Particles deposited onto duct bends, especially small diameter duct bends, can reduce the airflow rate and degrade the performance of the ventilation and air-conditioning system. The knowledge of predicting the particle deposition within ventilation ducts will be useful for improving the indoor air quality and the efficiency of the ventilation and air-conditioning system.

Over the past few decades, several studies have been conducted to investigate the particle deposition. Pui et al. investigated the deposition efficiency of liquid particles in 5.03–8.51 mm diameter tubes of circular cross-section in both laminar and turbulent flow [2]. This experiment was carried out at constant flow Reynolds number (100, 1000, 6000, and 10,000). McFarland et al. conducted experiments similar to those of Pui et al. [3]. They performed physical experiments and simulations to investigate particle penetration through 45–180° bends with curvature Ratio of 2–10 in 16 mm diameter tubes. The simulations method used by McFarland et al. is Lagrangian simulations. With the help of Lagrangian simulations, particle penetration through bends was predicted, and it was found that there was good agreement between numerical and physical experiments. Unfortunately, both of those studies just focused on the duct bends with hydraulic diameters much smaller and air velocity much greater than those of typical ducts in HVAC. Additionally, the cross-sections of the bends in those studies are round rather than square.

Zhang and Ahmadi once studied particle transport and deposition in vertical and horizontal turbulent square duct flows in the presence of different gravity directions [4]. This study was performed with direct numerical simulation of the Navier–Stokes equation. It proved that particle deposition velocity varies with the direction of gravity. For horizontal ducts, with the effect of gravity, particle deposition velocity on the four surface of square duct is different. Following this study, Peters and Leith studied the mass distributions of the particles collected in a 20.3 cm-diameter, 90° bend with two ways of placement [5]. It should be mentioned that they regarded the bend as a whole rather than different four surfaces of the bend. This means that they neglected the difference of four surfaces of the bend. In addition, in the three-dimensional space, a bend can be placed in five ways rather than two, see section 2.4. However, in fact, in each way of placement, the deposition characteristics on the four surfaces are also different.

Particles that smaller than 10 μm are studied in most pervious works. However, recent study carried by Zhao and Wu brought

* Corresponding author. Tel.: +86 29 82202507; fax: +86 29 82202729.
E-mail address: Liag@xauat.edu.cn (A. Li).

0196-8904/$ - see front matter © 2011 Elsevier Ltd. All rights reserved.
doi:10.1016/j.enconman.2011.10.018

Nomenclature

a	cross dimension of the duct
C_{ave}	time-averaged airborne particle concentration in ventilation ducts
C_c	slip correction factor
C_{in}	time-averaged particle concentration at the inlet
C_{out}	time-averaged particle concentration at the outlet
d_p	particle diameter
D_h	hydraulic diameter of the duct
f	Fanning friction factor
J	time-averaged particle flux to the surface
k	fluctuation kinetic energy
L	duct section length
N_{dep}	particle deposition numbers to wall
N_{in}	total particle numbers in the inlet in the duct
$\bar{p}$	mean pressure
R_{ij}	Reynolds stress tensor
t	time
T	integral time scale
T_L	fluid Lagrangian integral time
u_i'	the ith fluctuation velocity component
u_i	instantaneous velocity
u	fluid phase velocity
u_p	particle velocity
u^*	friction velocity
V_d	deposition velocity
V_d^+	dimensionless deposition velocity
$\bar{u}_i$	mean velocity
U_{ave}	air average velocity in the duct
x_i	position

Greek symbols

ε	turbulence dissipation rate
λ	the mean free path of gas molecules
μ	molecular viscosity of the fluid (dynamic viscosity of air)
ρ	constant mass density (air density)
ρ_p	density of the particle
τ^+	dimensionless particle relaxation time
θ	angle of integral region

something new to the particle size selection [6]. They investigated the size distributions of particle deposited on ventilation duct in a room (4 m × 2.5 m × 3 m) with typical mechanical ventilation system. The air supply volume rate is 240 m^3/h and the corresponding air change rate is 8 air changes per hour (ACH). It reported that although the particles smaller than 10 μm are the majority in the air through the duct, the particles deposited on the duct surface are mostly larger than 10 μm. Our task group has studied the particle deposition in a horizontal turbulent duct flow simulated by different CFD (computational fluid dynamics) modeling [7], and deposition of particles larger than 10 μm (10–200 μm) was also predicted in vertical duct [8]. In these studies, we investigated the influence of drag, lift force, gravity, inertia force, turbulent diffusions, particle size and density, duct size and air velocity on particle deposition by Reynolds-averaged Navier–Stokes (RANS)-Lagrangian simulation. Preliminary studies suggest that the effect of lift force and gravity is significant with the particle larger than 10 μm, especially, with the particle larger than 40 μm. In this paper, we will discuss the deposition of particles ranging from 10 to 200 μm in a duct bend.

Over the past two decades, empirical equations, Eulerian and Lagrangian simulations were developed to predict particle deposition in turbulent flows on tube, pipe or duct surface. Lagrangian simulation is one of the main approaches to predicate the motion of particles in turbulent flow. Recently, Luo studied the particles deposition in a turbulent channel flow with direct numerical simulation (DNS) and Lagrangian simulation [9]; Zhang and Chen predicted the particle deposition onto indoor surfaces with Lagrangian simulation [10]. In both of the two studies, the results of Lagrangian simulation of particle deposition are consistent with the result of experiment and direct numerical simulation in both magnitude and tendency. It means Lagrangian simulation is an effective method to investigate the particle motion in the turbulent flows. In this study, we use Lagrangian simulation to predict the deposition velocity of particles in smooth duct bends flow. Drag, lift force, gravity, inertia force and turbulent diffusions are taken into account in this simulation. The influence of particle size, relaxation time, air velocity and duct placement is also discussed. In order to validate particles deposition behavior and mechanism, multiple comparisons are made between the predicted result and the previous studies, which is summarized in Table 1.

Based on the analyses above, we select the ventilation square duct bend with cross-section of 0.3 m × 0.3 m. Two kinds of air velocities of 3.0 m/s and 7.0 m/s are adopted. It should be noticed that particle deposition characteristics on the four surfaces of the bend in five ways of placements are firstly reported in this paper, and it brings a whole new insight on particles deposition behavior in duct bends.

2. Numerical method

In this study, we adopt the one-way coupling lagrangian eddy lifetime model, at different air velocities of 3.0 m/s and 7.0 m/s to predict the deposition rates of the particles. Dimensionless deposition velocities of particles for 10, 15, 20, 30, 40, 50, 70, 80, 100, 120, 150, 180 and 200 μm are predicted in turbulent flows with developed velocity profiles in smooth square ventilation duct bends. We choose the ventilation duct bend with cross-section of 0.3 m × 0.3 m, which is the most typical duct in the HAVC systems. And the Lagrangian approach also splits the particle phase into a separately set of individual particles and tracks these particles separately through the flow domain by solving the equations of particle movement. It employs the following assumptions:

(1) No particle rebounds on solid walls.
(2) No particle coagulates in the particle deposition process.
(3) All particles are in spherical solid shape.

The turbulence model in this simulation is Reynolds stress transport model (RSM), and turbulent diffusion model and eddy lifetime model are introduced to simulate dispersion phase. Taking into account the lift force, gravity, inertia force, drag and turbulent diffusions, the simulation analyzes the influence of all these factors on the deposition velocities of the particles. It should be noticed that lift force was first derived by Saffman [11]. In their study, Saffman found that a particle entrained in a shear flow field may experience a force perpendicular to the main flow direction. The force was named Saffman lift force.

This study use commercial computational fluid dynamics (CFD) software, FLUENT™ (version 6.3) to predict both air motion and particle deposition. FLUENT™ now is one of the most widely used CFD software that contains broad physical modeling capabilities. In

Table 1
Summary of conditions in particle deposition studies.

Investigator	Duct			Particle				Methods	References
	Deposition surface	D_h (cm)	Re ($\times 10^3$)	Material[a]	ρ_p (g/cm^3)	d_p (μm)	τ^+ (–)		
Present study	Smooth square duct bend with five different ways of placement	33.9	34–365		1.5	10–200	4–1482	Lagrangian simulations	
Zhang et al.	Smooth square horizontal duct	33.9	56–142		1.5	10–200	7–1300	Lagrangian simulations	[7]
Wu and Zhao	Smooth square horizontal duct	45.14	37–263		10	0.01–100	NR	Eulerian model	[18]
Peters and Leith	Smooth glass bend	20.3	368	Glass beads	2.45	5–25	NR	Experiment	[5]
Zhang and Ahmadi	Vertical channel wall and horizontal channel floor	NR	8		1.12–2.24	0.01–50	10^{-5}-100	Lagrangian simulations	[4]
McFarland et al.	Round wax tube bends	1.6	3–20	Oleic acid	0.89	10	0.4–37	Experiment	[3]
Uijttewaal and Oliemans	Vertical pipe wall	5	5.3–42		1.2	3.6–940	5–4800	Lagrangian simulations	[16]
Pui et al.	Round stainless steel and glass tube bends	0.50–0.85	6–10	Oleic acid	0.89	1.0–7.0	0.4–25	Experiment	[2]
Liu and Agarwal	Round glass tube	1.27	10–50	Olive oil	0.92	1.4–21	0.21–770	Experiment	[21]
Sehmel	Round aluminum tube	0.53–7.14	4.2–61	Uranine-methyl blue	1.5	1.0–28	0.04–29	Experiment	[22]

NR = not reported.
[a] In the Lagrangian simulations and Eulerian model, the particles are all virtual sphere, having no material.

particle deposition simulation, the predicted results of the software have been thoroughly validated over the ranges of parameters that encountered in this study [12].

2.1. Simulation of the turbulent airflow field

2.1.1. Turbulent airflow model

The air in the ventilation ducts can be regarded as a three-dimensional, incompressible, stable, isothermal, turbulent and continuous fluid, which is governed by conservation laws of mass and momentum, and continuity equations and momentum conservation equations for the mean motion of the particles are as follows:

$$\text{Continuity equation}: \frac{\partial \bar{u}_i}{\partial x_i} = 0 \tag{1}$$

$$\text{Momentum conservation equations}: \bar{u}_j \frac{\partial \bar{u}_i}{\partial x_j} = -\frac{1}{\rho}\frac{\partial \bar{p}}{\partial x_i} + \frac{\mu_t}{\rho}\frac{\partial^2 \bar{u}_i}{\partial x_j \partial x_j} - \frac{\partial}{\partial x_j} R_{ij} \tag{2}$$

where $\bar{u}_i$ is time averaged mean stream-wise air velocity, x_i is the position, ρ is the constant mass density (air density), μ is the dynamic viscosity, μ_t is the turbulent viscosity, and $R_{ij} = \overline{u_i' u_j'}$ is the Reynolds stress tensor. Here, $u_i' = u_i - \bar{u}_i$ is the ith fluctuation velocity component.

The transport equations in turbulence mentioned above were introduced by Daly and Harlow [13]. In previous studies, these equations were described in detail and their applicability was also demonstrated by comparison of solution with experiments. Following this study, Launder et al. developed a model of turbulence named Reynolds's stress model (RSM) in which the eddy viscosity approach was discarded and the Reynolds stresses were directly computed [14]. Here, the writer adopts the RSM as the turbulence model to close those equations by solving Reynolds stress, together with an equation for the dissipation rate.

2.1.2. Boundary conditions

The boundary conditions of developed flow in the simulation at the inlet and outlet are velocity-inlet and pressure-outlet boundary conditions. A fully developed velocity profile is supplied at the inlet. The walls of the bend are smooth and no-slip boundary conditions are employed to them.

2.2. Dispersion phase model

2.2.1. Turbulent diffusion model of the particle

The turbulent diffusion model of the particles in the Lagrangian simulations can provide more accurate information of the system while considering turbulent diffusion of particles and poly-disperse system and mono-disperse system having different air velocities, temperatures and particle sizes.

Fluent introduced the concept of the integral time scale, T, in the prediction of particle dispersion [12]. Integral time scale indicates the time spent in turbulent motion along the particle path, and can be given as:

$$T = \int_0^\infty \frac{u_p'(t) u_p'(t+s)}{\overline{u_p'^2}} ds \tag{3}$$

The integral time is proportional to the particle dispersion rate, as larger values indicate more turbulent motion in the flow. For small "tracer" particles that move with the fluid (zero drift velocity), the integral time becomes the fluid Lagrangian integral time, T_L. When the Reynolds stress model (RSM) is used, this time scale can be approximated as,

$$T_L \approx 0.3 \frac{k}{\varepsilon} \tag{4}$$

2.2.2. Eddy lifetime model

Eddy lifetime model of particles is the Lagrangian stochastic model which can be used to trace the trajectory of the particle in the duct flow. This model is introduced by Graham and James, who investigated the relationships of the eddy time, length scales and certain integral scales in homogeneous isotropic stationary turbulence (HIST) [15]. After setting the initial conditions that define the starting positions, velocities and sizes, the motion of single particle can be computed, and during this process, the particle is assumed to interact with a turbulent eddy which possesses a specific size, lifetime and velocity.

The particle is assumed to interact with the fluid phase eddy over the smaller of the eddy lifetime and the eddy crossing time. And when this time is reached, a new value of the instantaneous velocity can be obtained by recomputation. This model has been applied widely for its simplicity and high computational efficiency, especially for the satisfactory results while employed to the complex flow.

2.2.3. Initial and boundary conditions of the particle

The primary input for the particle phase calculations are the initial conditions that include the starting positions, velocities and particle sizes. In this study, it is assumed that 10^6 discrete particles whose diameter rang from 10 to 200 μm are released into the duct and are distributed uniformly at the entrance cross. The density of the particle is specified as 1500 kg/m^3.

The air and particle are assumed at 25 °C with an atmospheric pressure (101,325 Pa). Particle concentrations in HVAC ducts are supposed to be low enough to ignore interaction between particles. The surface of the duct is postulated to be a perfect sink so that once a particle contacts the wall, it will instantly adhere to the wall rather than bounce or detach. This assumption is according to the study of Uijttewaal and Oliemans who investigated the particle dispersion and deposition in vertical pipe flows with direct numerical and large eddy simulations [16].In their study, good agreement was observed between their predicted results and the experiment results with this assumption.

2.3. Calculation of particle deposition rates

Deposition rates are most commonly studied in the form of the dimensionless deposition velocity versus the dimensionless relaxation time.

2.3.1. Dimensionless particle deposition particle

The dimensionless particle deposition velocity is defined by normalizing the dimensional deposition velocity with the friction velocity:

$$V_d^+ = \frac{V_d}{u^*} \tag{5}$$

where V_d^+ is the deposition velocity, u^* is the friction velocity.

The deposition velocity, V_d, of a particle to a duct surface is defined as

$$V_d = \frac{J}{C_{ave}} \tag{6}$$

where J is the time-averaged particle flux to the surface and C_{ave} is the time-averaged airborne particle concentration in the duct, usually evaluated at the centerline of the flow.

The friction velocity of turbulent duct flows.

The expression of u^* is given by Anand et al. who derived u^* in order to calculate particle penetration through aerosol transport lines [17]. u^* is defined as:

$$u^* = U_{ave}\sqrt{f/2} \tag{7}$$

where f is the Fanning friction factor, which is given by

$$\frac{1}{\sqrt{f}} = -3.6\log\left[\frac{6.9}{\mathrm{Re}} + \left(\frac{k}{3.7D_h}\right)^{1.11}\right] \tag{8}$$

where Re is Reynolds number of the duct flow, based on the average flow velocity and the hydraulic diameter of the duct:

$$\mathrm{Re} = \frac{D_h U_{ave}}{v} \tag{9}$$

here v is the kinematic viscosity of air, D_h is the hydraulic diameter of the duct, is defined as:

$$D_h = \frac{4A}{p} \tag{10}$$

here A is the cross-sectional area of the duct and P is the perimeter of a section through the duct, normal to the direction of flow.

In this study, the turbulent flow in the smooth ventilation duct bends is developed, so we calculate the Fanning friction factor f by applying Eq. (8). $V_{d,total}$ is defined as the deposition velocity which is determined as area-weighted average over all interior duct surfaces. Wu and Zhao studied the effect of ventilation duct as a particle filter by modeling particle deposition in ventilation ducts [18]. In that study, they derived the $V_{d,total}$ applied to straight duct. According to their deduction, we can derive $V_{d,total}$ applied to square duct bend. The derivation is given in Appendix A. The deposition velocities to the surface of the duct bend can be calculated as:

$$V_{d,total} = -\frac{U_{ave}\cdot \ln\frac{C_{out}}{C_{in}}}{3\pi} \tag{11}$$

If the particle penetration coefficient P through ventilation duct is defined as the ratio of out duct particle concentration over in duct particle concentration, this coefficient, with the assistance of Eq. (12), could be expressed as

$$P = \frac{C_{out}}{C_{in}} = \exp\left(\frac{-3\pi\cdot V_{d,total}}{U_{ave}}\right) \tag{12}$$

and the particle deposition coefficient D can be calculated as

$$D = 1 - P = 1 - \exp\left(\frac{-3\pi\cdot V_{d,total}}{U_{ave}}\right) \tag{13}$$

2.3.2. Dimensionless particle relaxation time

The dimensional relaxation time of a particle, τ_p, is the characteristic time for a particle velocity responding to changes in air velocity. It may be calculated for particles in the Stokes flow regime as follows:

$$\tau^+ = \frac{C_c\rho_p d_p^2 u^{*2}}{18\mu v} \tag{14}$$

where C_c is the Cunningham slip correction factor, ρ_p is the particle density, d_p is the particle diameter and μ is the dynamic viscosity of air. The slip correction factor can be estimated by the expression:

$$C_C = 1 + \frac{2\lambda}{d_p}(1.257 + 0.4e^{-(1.1d_p/2\lambda)}) \tag{15}$$

where λ is the mean free path of gas molecules.

In addition, the dimensionless particle relaxation time is conducted based on the hypothesis of Stokes flow regime. But previous studies have proved that it also can be used in the flow with high Reynolds number [19,20].

2.4. Calculation region and grid generation

In this study, the bend size is 0.3 m × 0.3 m. the bend ratio is 1.5, and bend angle is 90°. It is a typical duct bend in heating, ventilation and air-conditioning (HVAC) systems. In the three-dimensional space, a bend have five different ways of placement. The five ways of placements are named from Cases 1 to 5, and the four surfaces are named from Surfaces 1 to 4, see Fig. 1.

Flow velocity profiles in ducts are developed. Velocity field of developed flow is calculated at two air velocities of 3.0 m/s and 7.0 m/s, respectively, and as the duct is selected properly, the research objects will not only accord with the size requirement of ventilation duct, but also avoid the velocity of the air being too fast. The configuration of the computer applied is as follows: EMS memory is 4 GB, CPU is 5.2 MHz and HD capacity is 500G.

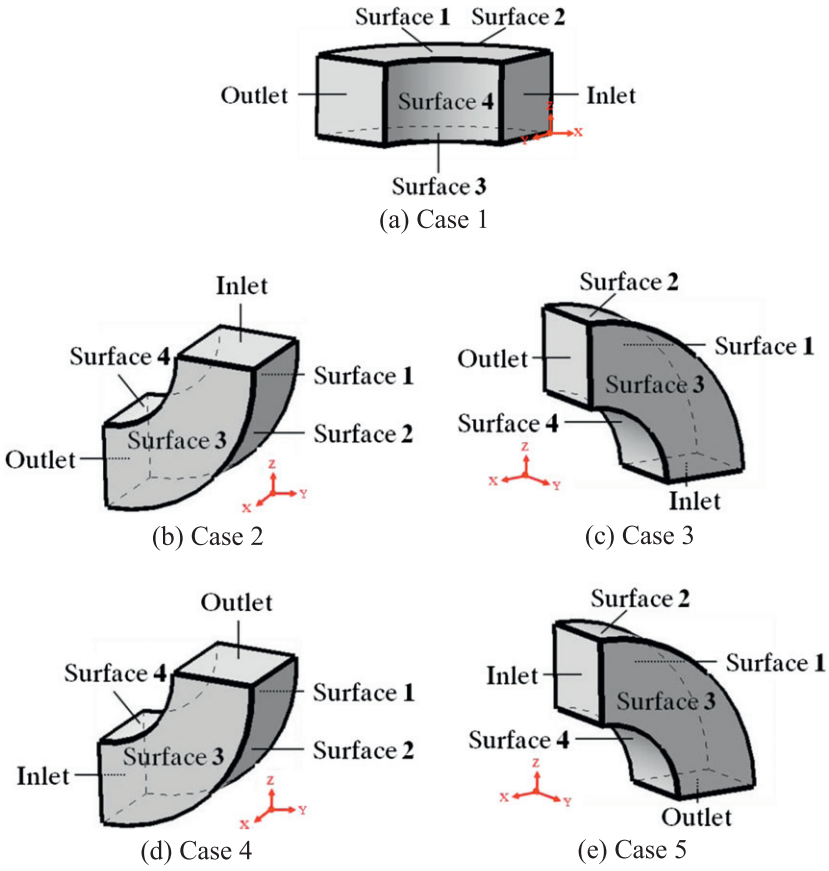

Fig. 1. Placement of ventilation duct bends.

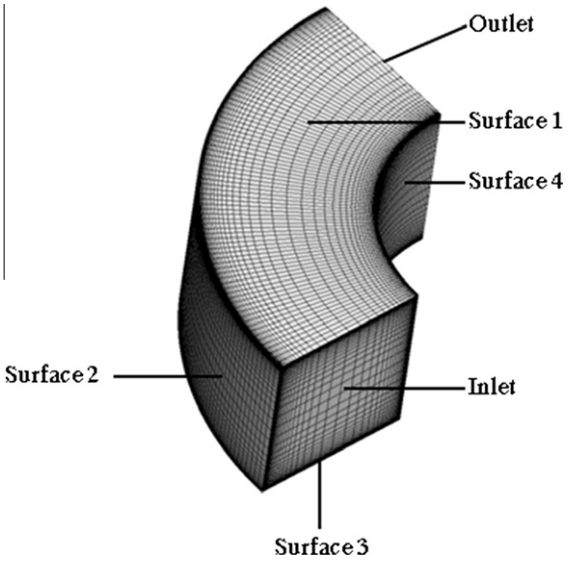

Fig. 2. Grid generation and surface number.

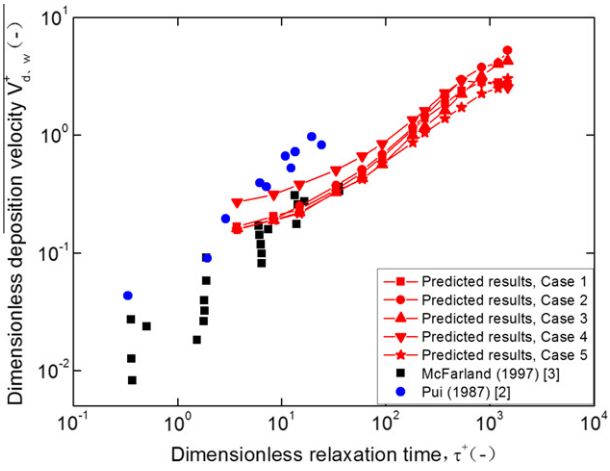

Fig. 3. Comparison of dimensionless deposition velocities in 90° bend duct predicted in five cases with the data of Pui et al. and McFaland et al.

Because the velocity gradient becomes larger on the fluid approaching the duct wall, we refine the mesh there, see Fig. 2. Grid independence study is introduced in this paper. Nine kinds of grids with different grid number of 1×10^4, 5×10^4, 8×10^4, 1×10^5, 5×10^5, 8×10^5, 1×10^6, 5×10^6, and 8×10^6 are used to predict the dimensionless particle deposition velocity. The difference of the predicted results is found to be minor for grid number from 8×10^5 to 10^6. Furthermore, there is no difference between the predicted results with the grid number of 1×10^6, 5×10^6, 8×10^6. Hence in the present simulation, the grid number is 10^6.

Each surface of the duct is numbered, and five cases are studied according to the direction of the gravity in order to investigate the particle deposition of each surface of the duct bend which has different way of placement. The number of the surface can be determined by left hand rule: if the fingers of the left hand are placed around the wire, the thumb will point in the direction of the outlet, and other fingers of the left hand curl around the duct in the direction of the number sequence. The intrados, which can be regarded as reference surface, is numbered as Surface 4.

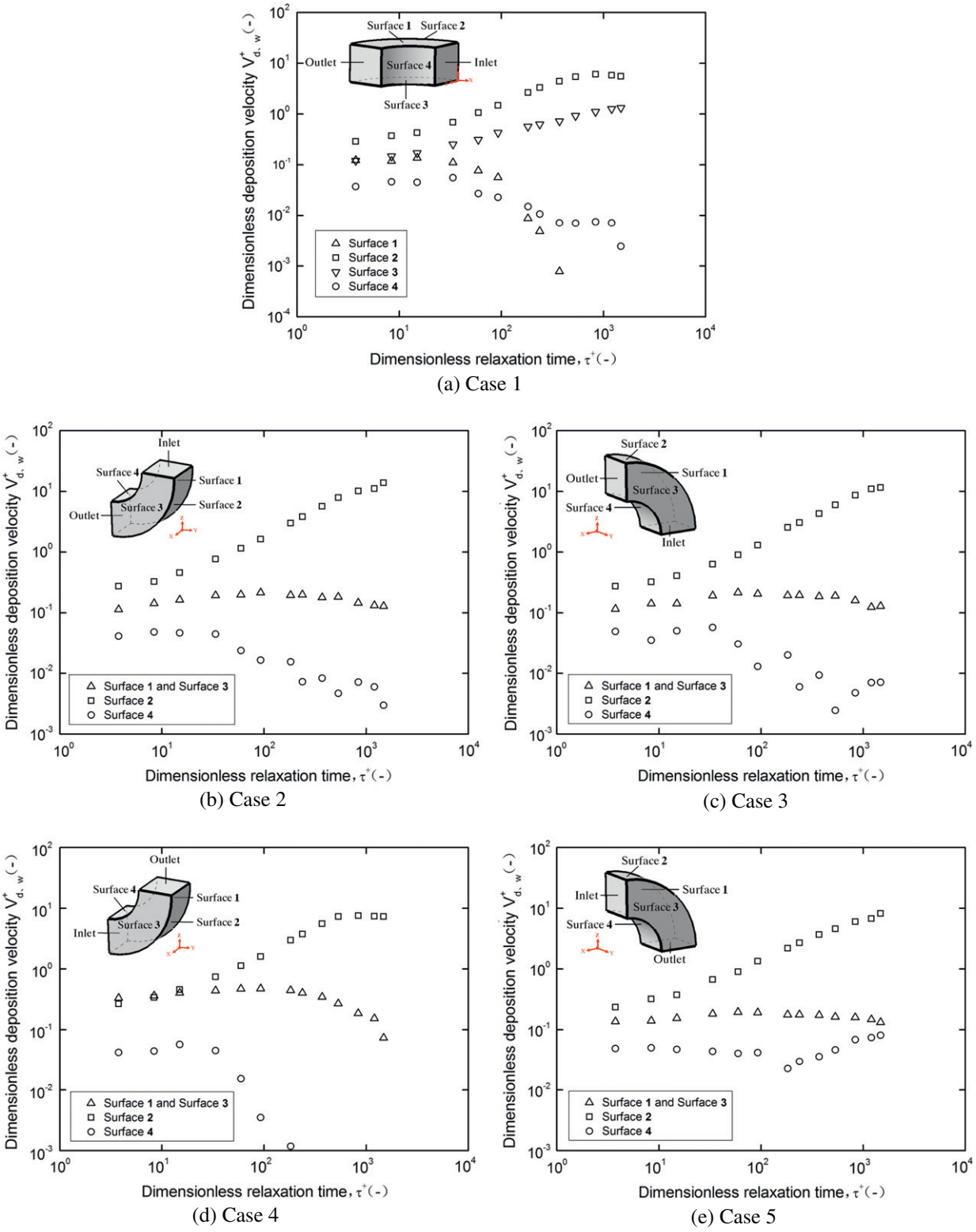

Fig. 4. Dimensionless deposition velocity onto each surface of the bend at air speed of 7.0 m/s.

3. Results

3.1. Particle deposition in duct bends with different dimensionless relaxation time

Particle deposition in turbulent flow is commonly studied through investigating the relationship between dimensionless particle deposition velocity and dimensionless particle relaxation time. The dimensional relaxation time of a particle is the characteristic time for a particle velocity to respond to a change of air velocity, see Eq. (14). Here, we discuss the impact of dimensionless relaxation time on dimensionless particle deposition velocity through comparing predicted results with experimental results from Pui et al. [2] and McFaland et al. [3], see Fig. 3.

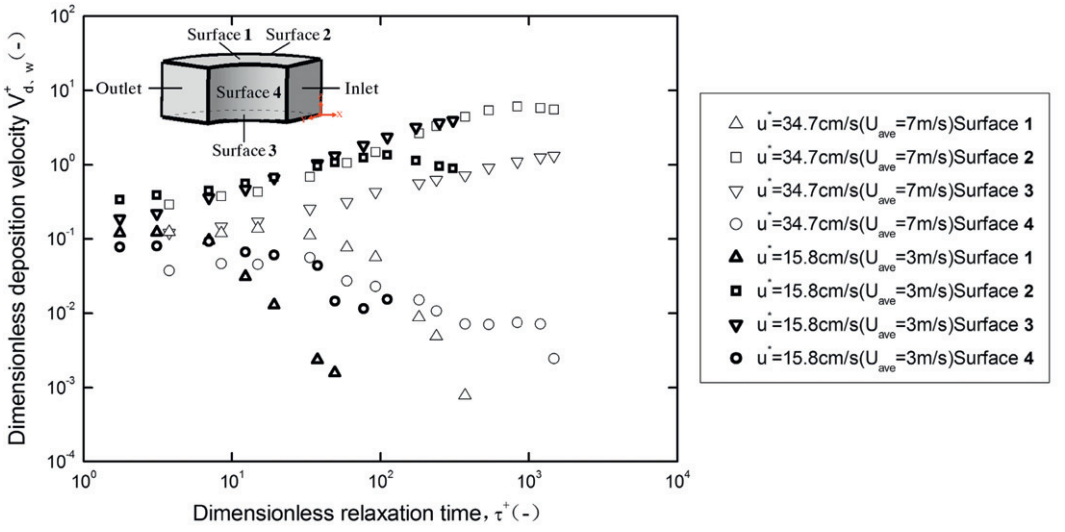

(a) Case 1

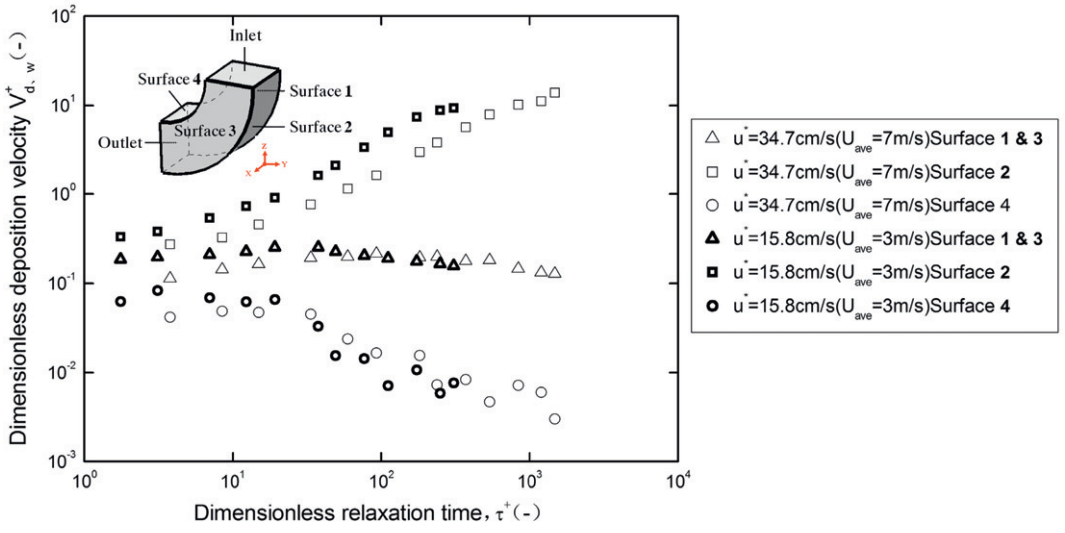

(b) Case 2

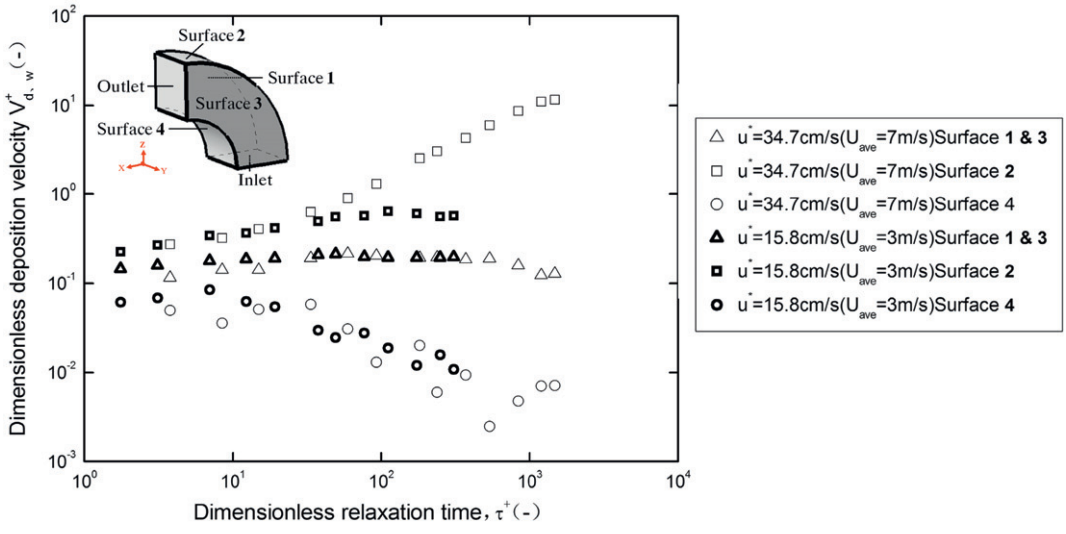

(c) Case 3

Fig. 5. Dimensionless deposition velocity to each surface of the duct bends at two air speeds of 3.0 m/s and 7.0 m/s.

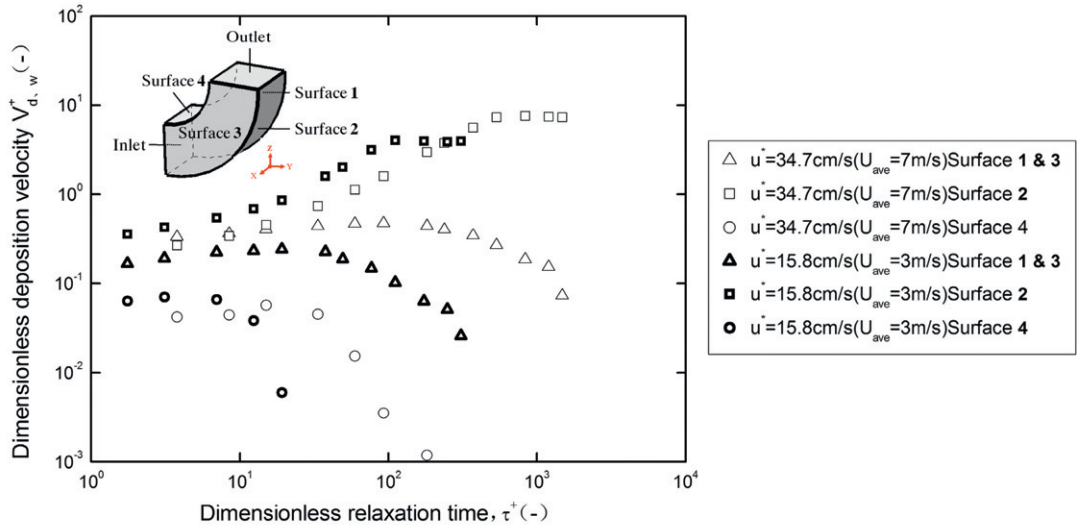

(d) Case 4

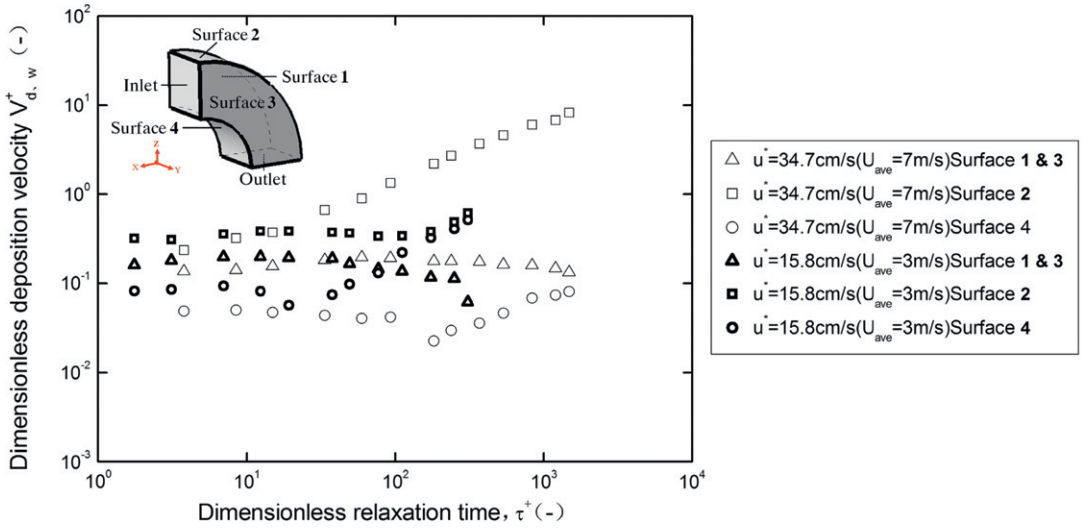

(e) Case 5

Notes: In case 1, we discuss surface 1 and surface 3 respectively, while in case 2-5, because the duct is plane-symmetric, and surface 1 and surface 3 are identical and both parallel with gravity, we discuss these two surfaces together as surface 1&3.

Fig. 5 (*continued*)

Dimensionless relaxation time from experimental results of Pui et al. [2] and McFaland et al. [3] is ranging from 0.33 to 36.06, while that of the our study is ranging from 3.76 to 1482.87. Data connection is made and good agreement can be observed with McFaland et al. [3], Pui et al. [2] and predicted results in five cases. In all of cases of this study and experiment conducted by Pui et al. [2] and McFaland et al. [3], the dimensionless deposition velocities of the ventilation duct increase as the dimensionless relaxation time increases. This phenomenon can also be seen in the studies of Peters and Leith [5] and Wu and Zhao [18].

3.2. Particle deposition in duct bends with different placement

In HVAC system, the placements of bend are various, and thus lead to different particle deposition pattern of each surface of the bend. In this study, the particle deposition velocity in the 90°bend whose bend ratio is 1.5 and cross-section is 0.3 m × 0.3 m is simulated in five cases stated above at air velocity of 7.0 m/s using RSM-Lagrange simulation, and the simulation results are illustrated in Fig. 4.

Although at large air velocity of 7.0 m/s, the dimensionless deposition velocity to surface 2 changes slightly according to the placement of the duct bends, for $3.76 < \tau^+ < 1482.87$, it is always the highest velocity compared with those to other surfaces (Fig. 4). In addition, the velocity to Surface 2 increases significantly as the dimensionless relaxation time increases, and it is important to note that in Case 1 and Case 4, the velocity stop increasing when the dimensionless relaxation time increases up to about 1000, see Fig. 4a–b.

In Case 1, the placement of the duct bend leads to different dimensionless deposition velocities to each surface, see Fig. 4a. For $3.76 < \tau^+ < 1482.87$, putting them in an order according to their magnitude, the dimensionless deposition velocity to surface 2 is the highest, and then is that to surface 3, and that to surface 1

and 4 become the lowest alternatively when the dimensionless relaxation time increase. The dimensionless deposition velocity to surface 3 increases as the dimensionless relaxation time rises, whereas the velocity to surface 1 decreases during that process, and this is similar to the change tendency in the straight duct, see Figs. 7 and 8.

In Cases 1–4, dimensionless deposition velocity to surface 4 always decreases as the dimensionless relaxation time increases, see Fig. 4a–d. However, in Case 5, it firstly decreases as the dimensionless relaxation time increases and then increases after τ^+ increasing up to 181, Fig. 4e.

In Cases 2–5, we discuss the particle deposition on surface 1 and 3 for the conditions of the two surfaces are the same, see Fig. 4b–e. For $3.76 < \tau^+ < 100$, as τ^+ increases, the dimensionless deposition velocity increases, while for $\tau^+ > 100$, the dimensionless deposition velocity decreases with τ^+ increasing, which is similar to the change tendency of the dimensionless deposition velocity to the wall of the rectangular straight horizontal duct, see Fig. 6.

3.3. Particle deposition velocity at different air velocities

Air velocity is also a key factor in particle deposition research, and there are a lot of researchers investigating the particle deposition in straight duct. Summary of the conditions in those studies can be seen in Table 1. In order to understand the influence of air velocity on particle deposition, we study the particle deposition in the duct bend with five placements at two air velocities of 3.0 m/s and 7.0 m/s using RSM-Lagrange simulation. The simulation results are show in Fig. 5.

At different air velocities, the dimensionless deposition velocity to surface 2 is not always higher than that to other surfaces. In Cases 2 and 4, the velocity to surface 2 increases as the air velocity increases and maintain the highest among the velocities of all the surfaces at both air velocities, while in Cases 3 and 5, the velocity to surface 2 at air velocity of 7.0 m/s is lower than that at air velocity of 3.0 m/s, see Fig. 5b–e.

In Case 1, for $3.76 < \tau^+ < 307.91$, the change of air velocity leads to the change of particle deposition velocity to the four surfaces of the duct bend. First, the dimensionless deposition velocities to surface 2 and 3 are always higher than those to surface 1 and 4 at different air velocities. Second, although at high air velocity, such as 7.0 m/s, the dimensionless deposition velocity to surface 2 is higher than that to surface 3, at low air velocity, such as 3.0 m/s, it is lower than that to surface 3. Finally, for surface 1, dimensionless deposition velocities increase as the air velocities increase, while for surface 4, the velocities slightly increase as the air velocities increase, see Fig. 5a.

In Cases 2 and 3, for $3.76 < \tau^+ < 307.91$, as the air velocities change, dimensionless deposition velocities to surface 1, 3 and 4 do not change significantly, which are different from those in other cases, see Fig. 5b–e.

In Cases 4 and 5, dimensionless deposition velocities to surface 1 and 3 increase as the air velocities increase for $3.76 < \tau^+ < 307.91$. Further, in Case 4, the velocity to surface 4 increases as the air velocity increases, and in Case 5, an interesting phenomenon appears that there is a inflexion in the change curve of dimensionless deposition velocity to surface 4, and this inflexion tends to move toward left as the air velocity becomes lower, see Fig. 5d–e.

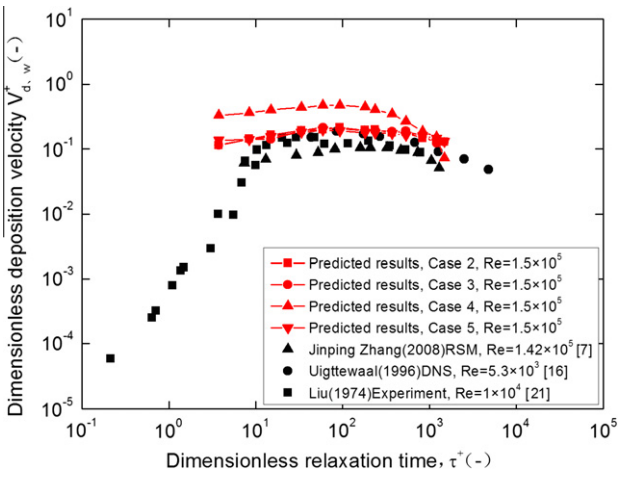

Fig. 6. Comparison of dimensionless deposition velocities to surface 1 and 3 of 90° bend duct predicted in four cases with the data of Liu and Agarwal, Uijttewaal and Oliemans and Zhang et al.

4. Discussions

4.1. Effect of gravity on dimensionless deposition velocity

In Cases 2–5, because the duct is plane-symmetric, and surface 1 and surface 3 are identical and parallel with gravity, and we discuss these two surfaces together as surface 1 and 3. The Experiment of Liu and Agarwal is used here for validation [21]. Detail information of that study can be seen in Table 1. After comparing the predicted results with the previous research which studied the change of dimensionless wall deposition velocity in the straight horizontal duct, we find that the predicted results well agree with previous research, see Fig. 6. For smaller particles ($3.76 < \tau^+ < 100$), interactions with near-wall eddies are potentially important in determining deposition velocities, however, for larger particles ($100 < \tau^+ < 1482.87$), the particles are too large to respond to the rapid fluctuations of near wall eddies and transport to the wall by turbulent diffusions very weak, and thus they reach the wall through momentum imparted by large eddies in the core of the turbulent flow. Meanwhile, the dimensionless deposition velocity in predicted data are larger than the data of previous research, this might because the flow in the duct bend is more turbulent than that in the straight duct.

As we know, the density of air is so small that we can ignore the gravity and inertia force of the air, however, these of the particles cannot be neglected due to the relatively high density of particles. The gravity and inertia force of particle plays a very important role in particle motion. On one hand, the gravity permanently applies a vertical downward force on the particles which will accelerate or decelerate the particle velocity; on the other hand, the inertia due to the mass of the particles compels the particles to remain the previous motion and move in the tangential direction of the motion, in this study, toward surface 2.

In the process of particle deposition, gravity and inertia are very important as they are proportion to d_p^3, and so the effect of gravity and inertia force increase as dimensionless relaxation time rises, see Eq. (11). We study the effect of gravity on particle deposition through the relationship between dimensionless deposition velocity and dimensionless relaxation time. The Experiment of Sehmel is used here for comparison [22]. Detail information of that study can be seen in Table 1. In Case 1, surface 1 and 3 of the duct bend are equivalent to the ceiling and floor of the straight horizontal duct, so we can compare the change of the dimensionless deposition velocity to surface 1 and 3 with that to the ceiling and floor of straight horizontal duct, see Figs. 7 and 8. It is found that for $3.76 < \tau^+ < 1482.87$, the dimensionless deposition velocity to surface 1 decrease as the dimensionless relaxation time increases, and during this process, dimensionless deposition velocity to surface 3 rises. This phenomenon coincides well with the conclusion of dimensionless ceiling deposition velocity in straight horizontal

duct of previous research [7]. The conditions of the study can be seen in Table 1.The reason is that the gravity pointing to surface 3 and deviating from surface 1 will make the particle move toward surface 3 and away from surface 1.

4.2. Effect of inertia force on dimensionless deposition velocity

The inertia force will lead the particle move toward surface 2 and away from surface 4, which make the dimensionless deposition velocity to surface 2 higher than that to surface 4, especially at the air velocity of 7.0 m/s, when inertia force become the predominant force. In Case 1–5, for $3.76 < \tau^+ < 1482.87$, the dimensionless deposition velocity to surface 2 is always the highest, and in Cases 2–4 that to surface 4 is always the lowest. Further, the inertia force rises as the air velocity increases. We will talk about it in Section 4.3.

4.3. Effect of air velocity on dimensionless deposition velocity

The change of air velocity not only changes the turbulent flow in the duct bend, but also changes the inertia force imposed on the particles.

In Case 1, for $3.76 < \tau^+ < 307.91$, surface 2 and surface 3 are the major surfaces for particle deposition, and during the process of particle deposition, these two surfaces compete with each other for the particles. And so if one of them obtains more particles, the other will get less. The particle depositions on surface 2 and 3 are the result of combined action of gravity and inertia force. At high air velocity, such as 7.0 m/s, the inertia force of the particle is larger and become the dominant factor in particle deposition, so the dimensionless deposition to surface 2 is higher than that to surface 3, while at low air velocity, such as 3.0 m/s, gravity predominant the deposition process, and thus the velocity to surface 3 is higher than that to surface 2. This is the reason why dimensionless deposition velocity to surface 3 in bend increases as the dimensionless relaxation time increases, and in previous study, the dimensionless deposition velocity to floor of straight duct increases, see Fig. 7.

We cannot simply say that dimensionless deposition velocity to surface 2 always increases as the air velocity increases for it depends on the placement of the duct, such as in Cases 2 and 4. Although the combined action of gravity and inertia force having the same direction will enhance the particle deposition to surface 2, air velocity too high will take away the particles before they deposit, and thus lead to lower deposition velocity to surface 2 at high air velocity. On the contrary, if the directions of gravity and inertia force are opposite, high air velocity will intensify the particle deposition and make the deposition velocity increase, because the larger inertia force resulting from the higher air velocity will weaken the effect of gravity.

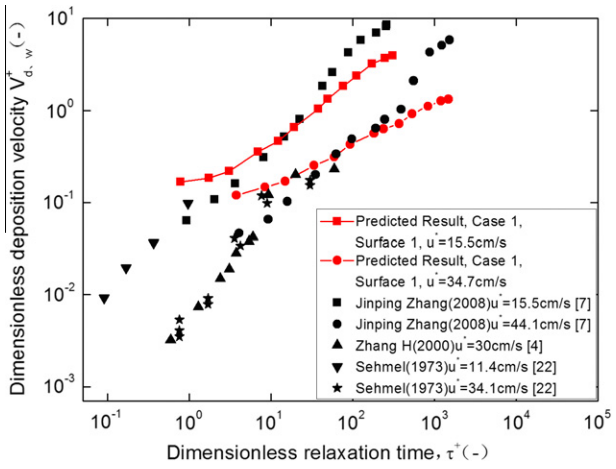

Fig. 7. Comparison of dimensionless deposition velocities to surface 1 of 90^0 bend duct predicted at two air velocities of 3 m/s and 7 m/s with the data of Sehmel, Zhang and Ahmadi and Zhang et al.

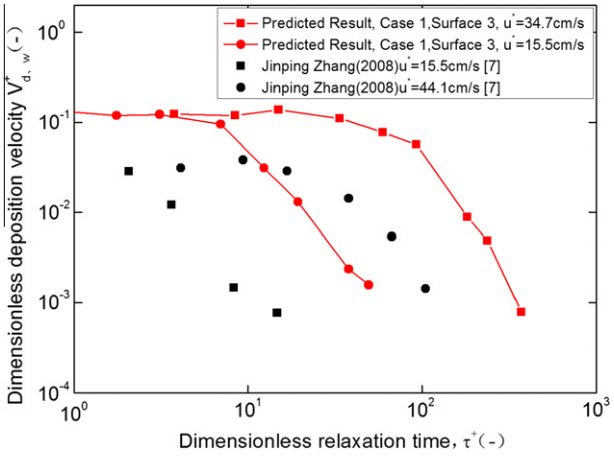

Fig. 8. Comparison of dimensionless deposition velocities to surface 1 and 3 of 90° bend duct predicted at four cases with the data of Zhang et al.

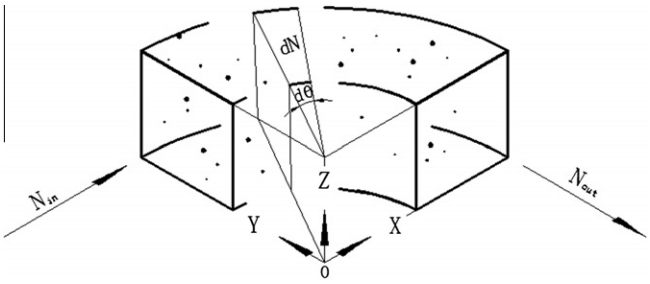

Fig. 9. Sketch map of the ventilation duct bend.

In Cases 2–5, surface 1 and 3 parallels with inertia force and gravity. As we talked about in section 4.1, In Cases 2–5, surface 1 and 3 of the duct bend are equivalent to the wall of the straight horizontal duct. When the air velocity increases, the Reynolds Number will become larger. This would increase the turbulence intensity of the duct flow, and thus enhance the turbulent diffusion, which will intensify the particle deposition onto surface 1 and 3.

In Case 5, because the gravity will enhance particle deposition on surface 2 when the inertia force weaken the deposition, there is a inflexion in the deposition curve of which τ^+ move from 181.93 to 12.36 as the air velocity decrease from 7.0 m/s to 3.0 m/s.

5. Conclusion

Deposition rates of particles ranging from 10 to 200 μm in smooth duct bends with developed velocity profiles based on the RSM (Reynolds stress transport model) at two air velocities of 3.0 m/s and 7.0 m/s are predicted by RANS-Lagrangian simulation. Drag, lift force, gravity, inertia force and turbulent diffusion are taking into account in this simulation and the influence of particle size, relaxation time, air velocity and placement is discussed. Results from this study give some new guidelines in particle deposition mechanism, as well as contribute to the discussion on combined effect of gravity and inertia force. The main results are as follows.

During the process of particle deposition in duct bends, gravity and inertia force all play very important roles: gravity permanently

applies a vertical downward force on the particles, and inertia force due to the mass of the particles compels the particles to remain the previous motion and move in the tangential direction of the motion, in this study, toward surface 2. Meanwhile, for $0.78 < \tau^+ < 1482.87$, the effect of gravity and inertia force increase as dimensionless relaxation time rises.

Surface 1 and 3 of the duct bend are equivalent to the ceiling and floor of the straight horizontal duct in Case 1, respectively, and equivalent to the wall of the straight horizontal duct in Cases 2–5. In Case 1, for $3.76 < \tau^+ < 1482.87$, change tendency of the dimensionless deposition velocity to surface 1 and 3 agree well with the result on ceiling and floor of straight horizontal duct, respectively. However, in Cases 2–5, for $3.76 < \tau^+ < 1482.87$, dimensionless deposition velocity to surface 1 and 3 in bend decreases as the air velocity increases due to the inertia force changes, and this does not agree with previous studies on the wall of the straight duct.

In Case 1, surface 2 and surface 3 compete with each other for the particle deposition. Higher air velocity leading to larger inertia force causes larger dimensionless deposition velocity on surface 2, while lower air velocity lead to larger dimensionless deposition velocity on surface 3 due to gravity. However, we cannot simply say that dimensionless deposition velocity to surface 2 always increases as air velocity increases for it depends on the placement of the duct. In Case 2 and Case 4, for $3.76 < \tau^+ < 307.91$, the combined action of gravity and inertia force having the same direction will enhance the particle deposition to surface 2. But air velocity too high will take away the particles before they depositing, and thus lead to lower deposition velocity to surface 2. On the contrary, if the directions of gravity and inertia force are opposite, high air velocity will intensify the particle deposition and make the deposition velocity increase, because the larger inertia force resulting from the higher air velocity will weaken the effect of gravity.

In Case 5, because the gravity will enhance particle deposition on surface 2 when the inertia force weaken the deposition, there is a inflexion in the deposition curve of which τ^+ move from 181.93 to 12.36 as the air velocity decrease from 7.0 m/s to 3.0 m/s.

Acknowledgements

This research project is sponsored by Natural Science Foundation of China (No. 50878177 and No. 50778145) and by the Research Fund for the Doctoral Program of Higher Education (No. 20106120110008).

Appendix A

The sketch map of the ventilation duct bends which is a in width and height is showed in Fig. 9. The area of the cross-section is equal to a^2, the area of the entire surface of the integral region is equal to $6a^2 d\theta$, and C_{in} and C_{out} represent the time-averaged particle concentration at the inlet and outlet, respectively.

Based on the assumption that the difference of the angle $d\theta$ (expressed in radians) is so small that time-averaged particle concentration in this volume can be regarded as uniform, within the period of time Δt, the conversation of mass can be given as follows:

$$-C \cdot V_{d,total} \cdot \Delta t \cdot 6a^2 \times d\theta = a^2 \cdot U_{ave} \cdot \Delta t \cdot dC \quad (16)$$

where C is time-averaged particle concentration, dC is the difference of the time-averaged particle concentration owing to particle deposition, U_{ave} is the bulk average air velocity in the duct.

Boundary conditions are:

$$\begin{cases} \theta = 0, & C = C_{in} \\ \theta = \frac{\pi}{2}, & C = C_{out} \end{cases}$$

Integrating between the limits yields:

$$\ln \frac{C_{out}}{C_{in}} = \frac{-3\pi \cdot V_{d,total}}{U_{ave}}$$

and the $V_{d,total}$ can be computed as:

$$V_{d,total} = -\frac{U_{ave} \cdot \ln \frac{C_{out}}{C_{in}}}{3\pi}$$

References

[1] Miguel António F, Reis A Heitor, Aydin Murat. Aerosol particle deposition and distribution in bifurcating ventilation ducts. J Hazard Mater B 2004;116:249–55.
[2] Pui DYH, Romay-Novas F, Liu BYH. Experimental study of particle deposition in bends of circular cross-section. Aerosol Sci Technol 1997;7:301–15.
[3] McFarland AR, Gong H, Muyshondt A, Wente WB, Anand NK. Aerosol deposition in bends with turbulent flow. Environ Sci Technol 1997;31:3371–7.
[4] Zhang H, Ahmadi G. Aerosol particle transport and deposition in vertical and horizontal turbulent duct flows. J Fluid Mech 2000;406:55–80.
[5] Peters Thomas M, Leith David. Measurement of particle deposition in industrial ducts. Aerosol Sci 2004;35:529–40.
[6] Zhao Bin, Wu Jun. Modeling particle fate in ventilation system—Part II: Case study. Build Environ 2009;44:612–20.
[7] Zhang Jinping, Li Angui, Li Desheng. Modeling deposition of particles in typical horizontal ventilation duct flows. Energy Convers Manage 2008;49:3672–83.
[8] Zhang Jinping, Li Angui, Zhang Jinping, Li Angui. Study on particle deposition in vertical square ventilation duct flows by different models. Energy Convers Manage 2008;49:1008–18.
[9] Luo Jianping. Simulation of Lagrangian dispersion using a Lagrangian Stochastic model and DNS in a turbulent channel flow. J Hydrodyn 2009;21:767–73.
[10] Zhang Z, Chen Q. Prediction of particle deposition onto indoor surfaces by CFD with a modified Lagrangian method. Atmos Environ 2009;43:319–28.
[11] Saffman PG. The lift on a small sphere in a slow shear flow. J Fluid Mech 1965;22:385–400.
[12] Fluent. Fluent user's guide, version 6.1. NH (USA): Fluent Inc.; 2003.
[13] Daly BJ, Harlow FH. Transport equations in turbulence. Phys Fluids 1970;13:2634–49.
[14] Launder BE, Reece GJ, Rodi W. Progress in the development of a Reynolds-stress turbulence closure. J Fluid Mech 1975;68(3):537–66.
[15] Graham DI, James PW. Turbulent dispersion of particles using eddy interaction models. Int J Multiphase Flow 1996;22:157–75.
[16] Uijttewaal WSJ, Oliemans RVA. Particle dispersion and deposition in direct numerical and large eddy simulations of vertical pipe flows. Phys Fluids 1996;8:2590–604.
[17] Anand NK, McFarland AR, Wong FS, Kocomoud CJ. EPOSITION: software to calculate particle penetration through aerosol transport lines. NUREG/GR-0006. US NRC final report; 1993.
[18] Jun Wu, Bin Zhao. Effect of ventilation duct as a particle filter. Build Environ 2007;42:2523–9.
[19] Ayse Sarimeseli. Sedimentation of particles in developed turbulent flow in rough pipes. Powder Technol 2002;127:144–8.
[20] Dmitry Eskin, John Ratulowski, Kamran Akbarzadeh. Modeling of particle deposition in a vertical turbulent pipe flow at a reduced probability of particle sticking to the wall. Chem Eng Sci 2011;66:4561–72.
[21] Liu BYH, Agarwal JK. Experimental observation of aerosol deposition in turbulent flow. Aerosol Sci 1974;5:145–55.
[22] Sehmel GA. Particle eddy diffusivities and deposition velocities for isothermal flow and smooth surfaces. Aerosol Sci 1973;4:125–38.